



## Hybrid testing to investigate higher mode effects in ductile designed RC shear walls

Hassan Fatemi<sup>1</sup>, Patrick Paultre<sup>2</sup>, Charles-Philippe Lamarche<sup>2</sup>

<sup>1</sup> Graduated Ph.D. Student, Department of Civil and Building Engineering, University of Sherbrooke - Sherbrooke, QC, Canada.

<sup>2</sup> Professor, Department of Civil and Building Engineering, University of Sherbrooke - Sherbrooke, QC, Canada.

### ABSTRACT

A hybrid testing programme was conducted to investigate the response of ductile reinforced concrete (RC) shear walls under earthquake ground motion. A test specimen corresponding to the base plastic hinge zone of an 8-storey shear wall was tested in a laboratory environment, whilst the remainder of the building structure was modelled numerically. The reference wall was scaled down by a factor of 1/2.75 to accommodate instruments and laboratory limitations. The RC wall was designed in accordance with the 2015 edition of the National Building Code of Canada (NBCC 2015) and the Canadian Standard Association A23.3-14 Code. Three earthquakes' time histories with different intensities were successively applied during the hybrid tests. The RC wall exhibited ductile behaviour under the design level and amplified ground motions, and flexural and shear cracks developed along the height of the plastic hinge region. According to the experimental results, the base shear force demand was amplified by a factor of 2.27 under the design level earthquake and by 3.01 under the high intensity earthquake. The decomposition of the displacements within the plastic hinge region into different deformation mechanisms showed that shear deformation governs the displacement at the top of the plastic hinge region when the maximum base shear force demand due to higher mode effects occurs. To evaluate the displacement ductility demand for the RC shear wall, hybrid tests were followed by a pushover test under a lateral force distribution equal to the square root of the sum of the squares of the first five modes. The shape of the lateral load distribution was calculated using a modal analysis of the structure in combination with the NBCC 2015 design spectra. The pushover test revealed that the tested ductile RC wall can withstand higher displacement ductility levels than those anticipated by NBCC 2015.

Keywords: Hybrid test, higher mode, RC shear wall, plastic hinge, displacement ductility

### INTRODUCTION

Most mid- and high-rise reinforced concrete (RC) buildings rely on RC structural walls as their seismic force resisting system. Ductile RC structural walls (commonly called shear walls) designed according to modern building codes are typically detailed to undergo plastic hinging at their base. Both the design moment envelope for the remaining portion of the wall and the design shear forces are evaluated based on the nominal or the probable flexural resistance of the wall in the plastic hinge region. Several analytical studies have shown that such designed structural walls can be subjected to shear forces in excess of the design values [1-5]. Plastic hinging can also develop in the upper portion of the walls. These effects are mainly attributed to higher mode response and are therefore more severe in taller or slender walls with long fundamental periods. The value of the fundamental period and the flexural overstrength at the wall base greatly affect the dynamic shear amplification and seismic force demands [6]. Alongside the effect of structural characteristics of RC shear walls, higher mode responses are further stimulated by intensive and high-frequency ground motions and hence may result in larger dynamic amplification effects.

Hybrid testing is an effective experimental method to study the natural behaviour of structures such as shear walls. The hybrid testing method enables the simulation of the seismic response of large structural elements such as RC shear walls without the need to include large masses typically encountered in multi-storey buildings. Hybrid simulations combine numerical models and experimental testing techniques using advanced control methods for the efficient and realistic evaluation of the seismic performance of structural elements. A given structural system is divided into two parts, a numerical and a physical substructure, and the discrete parts of the equation of motion for the whole structure are extracted from the relevant subassembly and then integrated. In this test method, the target displacements are applied in a quasi-static manner or in real time to the physical substructure, and the restored forces in the physical subassembly, measured experimentally, are fed back to the numerical model to continue the analysis in the next step. Figure 1 shows the concept of hybrid testing with substructuring.

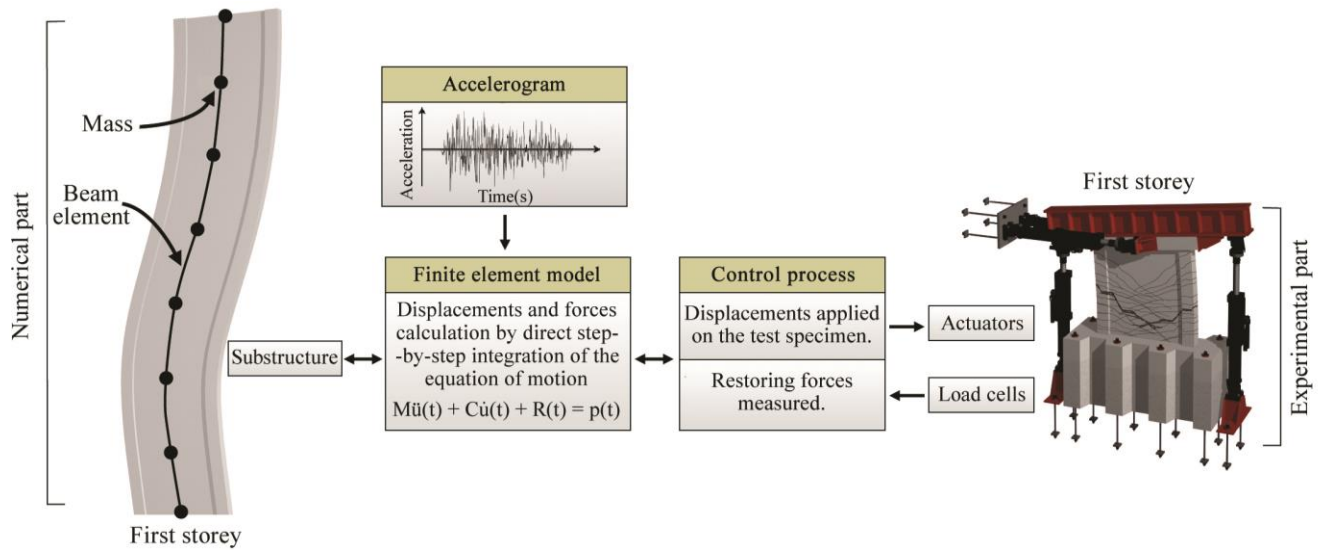


Figure 1. Hybrid test overall procedure and substructuring technic.

### TEST PROGRAMME

In this study, a test specimen corresponding to the base plastic hinge zone of an 8-storey RC shear wall was tested in the laboratory, whilst the remainder of the RC wall structure was numerically modelled using the OpenSees finite element package [7]. The reference wall was scaled down by a factor of 1/2.75 to obtain the dimensions of the test specimen. Hence, the test specimen was 1800 mm in length, including a 300 mm × 300 mm boundary element at each end, 2200 mm in height, and 160 mm in thickness. The RC wall was designed in accordance with the 2015 edition of the National Building Code of Canada (NBCC 2015) [8] and the Canadian Standard Association standard A23.3-14 [9]. The amplification of the base design shear force, accounting for the inelastic effects of higher modes specified by the CSA A23.3-14 standard [9], was not considered in order to experimentally evaluate it. Figure 2 presents the dimensions of the test specimen and the test set-up.

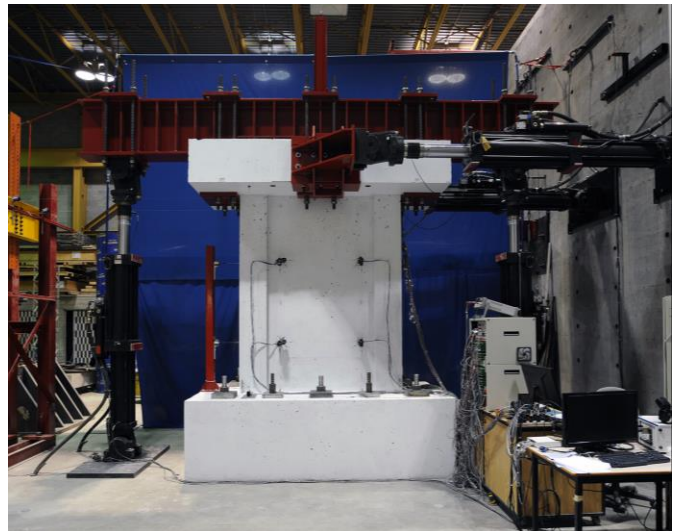
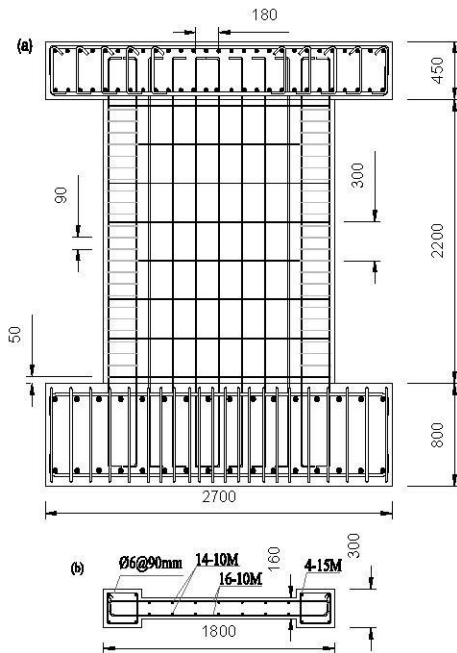


Figure 2. Test specimen dimensions and test set-up: Left (a) elevation of the specimen; Left (b) cross section of the test specimen; and Right: test set-up.

The ductile shear wall studied herein is the SFRS system of an 8-storey reinforced concrete building located in the Canadian city of Rivière-du-Loup, Quebec, on a soil type D. Seismic loads were determined considering the ductility related force modification factor  $R_d = 3.5$  and the overstrength related force modification factor  $R_o = 1.6$ . To achieve the most critical seismic effects, it was assumed that the reference wall has the maximum allowed fundamental period regarding the empirical equation given by NBCC 2015 [8] ( $T = 2 \times 0.05H^{3/4} = 1.2$  s). The storey masses were lumped at each storey level, and the Rayleigh period method [86, 173] was used to calculate the effective mass of the building for the fundamental period. A constant gravity load corresponding to  $0.03f'_cA_g$  was applied throughout the total duration of the tests, where  $A_g$  denotes the gross sectional area of the scaled RC wall and  $f'_c$  is the specified concrete compression strength. The RC shear wall was designed using a concrete with a specified compression strength of 30 MPa and steel reinforcements with specified yield strength of 400 MPa. Tension tests showed that the average yield and ultimate strength of the reinforcements are 460 MPa and 650 MPa, respectively. At the time of testing, the average compressive strength of the wall concrete was 28.6 MPa. The construction and test setup were built in the Structural Laboratory of the Civil Engineering Department of Université de Sherbrooke. Two different synthetic accelerograms generated by Atkinson [10] for Eastern Canada, where earthquakes generally have high frequency content, were used to carry out the hybrid tests. These earthquakes were scaled to match the uniform hazard spectra (UHS) of the city of Rivière-du-Loup, provided in NBCC 2015 [8]. Figure 3 shows the duration, order, magnitude, and definition of each excitation. The GM0 and GM2 excitations are the same histories but different intensities. Three degrees of freedom (DOF) at the top of the test specimen were controlled during the pseudo-dynamic hybrid tests, i.e., the horizontal and vertical translations as well as the rotation.

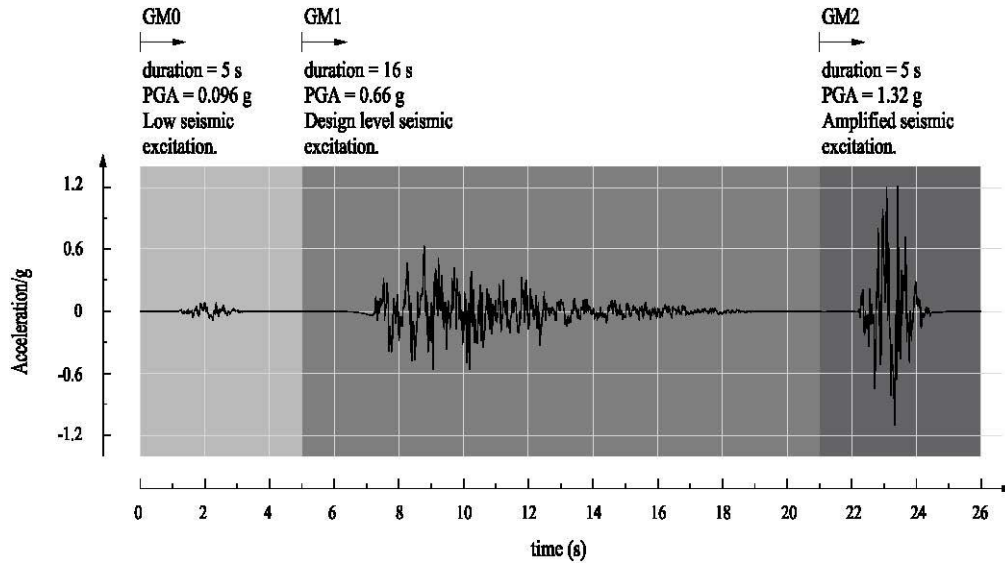


Figure 3. Applied seismic excitations.

The hybrid tests were followed by a pushover test under a lateral force distribution equal to the square root of the sum of the squares of the first five modes in order to evaluate the displacement ductility of the RC wall. The shape of the lateral load distribution was calculated using a modal analysis of the structure in combination with the NBCC 2015 uniform hazard design spectra.

## TEST RESULTS

### Hybrid tests

Figures 4a and 4b show the history of shear force and flexural moment demands at the base of the reference RC wall, respectively. The results showed that higher modes governed the behaviour of the RC wall mainly during two successive cycles under the GM1 design level seismic excitation. The maximum shear force during the higher mode vibrations under the design level seismic excitation was 770.5 kN (equivalent to 5825 kN shear force demand in the reference RC wall), occurred at time  $t = 3.876$  s from the beginning of the GM1 excitation. Despite a high shear force demand and considerable yielding of the horizontal reinforcement, no shear failure was observed under the design level earthquake (GM1). The maximum shear force and maximum flexural moment demands occurred at different times. Under the amplified seismic excitation GM2, maximum base shear demand was 1020 kN (equivalent to 7715 kN shear force demand in the reference RC wall). The maximum shear force and flexural moment demands occurred almost simultaneously, but no shear failure was observed.

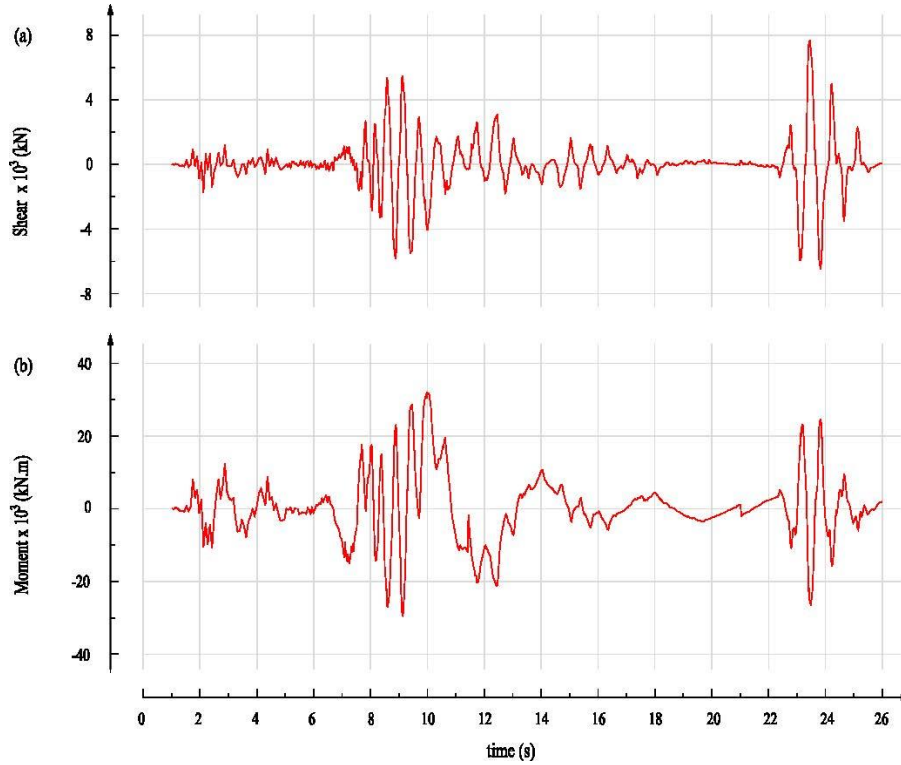


Figure 4. Seismic demands at the base of the reference RC wall: (a) shear force and (b) flexural moment.

The time of the maximum base shear force demand under the design level seismic excitation was 3.876 s from the beginning of the GM1, and the time of the first recorded yielding in horizontal reinforcements was 4.10 s from the beginning of the GM1. These values were compared, and it was concluded that due to higher shear forces and widening of shear crack openings, the contribution of the concrete to the shear resistance is reduced with an increase in the shear part taken by the reinforcements leading to yielding. Table 1 presents the seismic demands of the reference RC shear wall. The dynamic amplification factor of base shear force measured during the GM1 and GM2 ground motions are 2.27 and 3.01, respectively.

Table 1. Design and experimental forces for the reference RC shear wall.

	<u>Maximum moment</u>		<u>Maximum shear</u>	
	<u>Moment</u> <u>(kN.m)</u>	<u>Shear</u> <u>(kN)</u>	<u>Moment</u> <u>(kN.m)</u>	<u>Shear</u> <u>(kN)</u>
Capacity design	21000			2560
Design Earthquake (GM1)	32000	3725	22560	5825
Amplified Earthquake (GM2)	26160	7160	25725	7715

### Decomposition of the deformation mechanisms

To compare effects of different deformation mechanisms on the total displacement of the RC wall, the displacement of the specimen was decomposed into four deformation mechanisms:

$$U_T = U_{bs} + U_{bszr} + U_{sh} + U_{flex} \quad (1)$$

where  $U_T$  is the total lateral displacement at a given point;  $U_{bs}$  stands for the rigid motion due to sliding of the wall at the wall-foundation interface;  $U_{bszr}$  denotes the displacement due to the rotation from pull-out of the bars in tension;  $U_{sh}$  represents the displacement due to shear deformations; and  $U_{flex}$  represents the displacement due to flexural deformations. Test results showed that sliding of the foundation bloc with respect to the strong floor of the laboratory is negligible. It should be noted that only the 1445 mm externally instrumented section out of total 2200 mm height of the RC wall specimen provided data for extracting shear deformations. Thus, displacement analysis was performed at the level of 1445 mm above

the foundation. Displacements were decomposed at selected points in time. The time of the selected points during the GM1 excitation are 2.697 s, 3.027 s, 3.873 s (maximum shear demands), 4.431 s, and 4.986 s (maximum flexural moment demands) in the positive direction (pushing by horizontal actuators). On the negative side (pulling by horizontal actuators), times of 3.582 s, 4.122 s, 6.747 s, and 7.402 s were selected. Displacement history of the control point under the GM1 and GM2 seismic excitations are presented in Figures 5a and 5d, respectively. Figures 5b and 5c present the contribution of each source of deformation to the total displacement under the design level seismic excitation GM1. As it is clear from Figure 5b, the contribution of the shear deformations is initially marginal (less than 5%). At about the time that the maximum shear demand takes place ( $t = 3.876$  s from the starting point of the GM1 motion) shear deformations govern the response in contributing over 50% of the total displacement. When the maximum displacement response at the top of the specimen was reached, flexural deformations dominated the response, accounting for more than 60%. This caused the flexural crack openings to increase and the vertical reinforcements to yield, forming a plastic hinge at the base of the wall. At that time in the test, the concentrated rotation at the wall-foundation interface increased, contributing a larger portion of the total displacement. With an increase in the amplitude of the excitation yielding of the longitudinal reinforcements, it leads to an important increase in the flexural deformations. At the time corresponding to the maximum shear force demand, the flexural contribution is slightly more than 40%. Between the attainment of the maximum shear force demand and the maximum flexural moment demand, the relative share of the shear deformation drops significantly, and the flexural deformations increase. In the negative direction, as presented in Figure 5c, the flexural deformations govern the response of the RC wall from the beginning until the end. Between the selected times, the relative contributions are obtained by linear interpolations. These linear interpolations do not represent the exact contributions but provide a reasonable estimation [11].

Figures 5e and 5f show the contributions of the deformations in the lateral displacement under the GM2 excitation in the positive and negative directions, respectively.

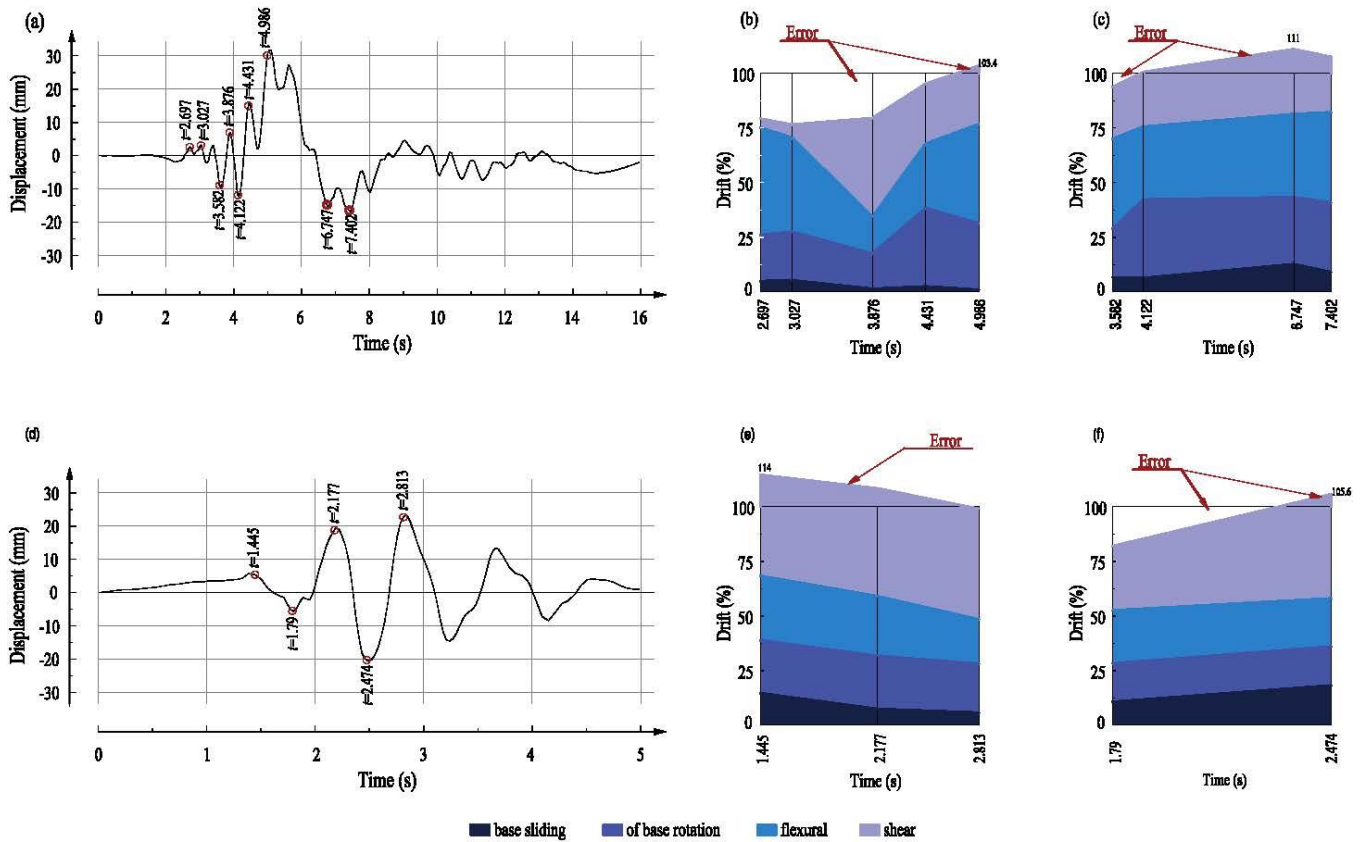


Figure 5. Displacement history of control point and displacement decomposition: (a) history under GM1; (b) decomposition in positive direction under GM1; (c) decomposition in negative direction under GM1; (d) history under GM2; (e) decomposition in positive direction under GM2; and (f) decomposition in negative direction under GM2.

It is obvious that in the positive and negative directions, the shear deformation has an important contribution in the response of the RC wall. Because the wall experienced severe yielding and wide crack openings during the GM1 excitation, the RC

wall exhibited a very soft behaviour, governed mainly by shear mechanisms in the positive and negative directions under the amplified excitation GM2.

The response of the test specimen to the low seismic excitation GM0 was within the linear elastic range of the materials. A visual inspection of the specimen after applying this excitation only revealed very few hairline cracks at the extremities of the base of the RC wall. After imposing design level excitation GM1 and the amplified excitation GM2, wide flexural and shear cracks could be found all over the wall's height. Figure 6 shows the crack pattern of the specimen after the GM1 and GM2 seismic excitations. No significant concrete crushing was observed at the extremities of the wall base. The outer longitudinal bars of the west (positive side) boundary element of the RC wall were slightly buckled. Because the concrete was mostly intact on both sides of the wall base, no visual investigation on the state of the confining bars in the boundary elements was possible.



Figure 6. Crack pattern of the test specimen: Left: at the end of GM1; and Right: at the end of GM2.

### Pushover test results

The maximum horizontal displacement at the top of the specimen during the pushover test was equivalent to a 2.5% drift. Nevertheless, the RC wall kept its structural integrity and vertical load carrying capacity. At displacements less than 15 mm in both positive and negative directions, the RC wall exhibited some torsional deformation. This is due the fact that the base of the wall was severely damaged, and the RC wall exhibited a very soft behaviour. This lack of stiffness alongside the delay between commands of the two horizontal actuators (one of the horizontal actuators was controlling the test by imposing the displacement to the specimen and the other one was enslaved to the first one) caused the specimen to twist. This phenomenon was not observed at absolute displacements greater than 15 mm. Figure 7 shows the overall hysteresis behaviour of the specimen in terms of the base shear force versus lateral displacement at the top of the specimen under the simultaneously applied cyclic displacements and rotations. Because the specimen was already heavily damaged after imposing the seismic excitations, the base shear force hysteresis curve begins with a very low rigidity until the cracks close on the compressive side, engaging interlock and friction along the cracks. The shear-displacement hysteresis presents a reverse S-shape. The area enclosed by the hysteresis loop is very small due to severe pinching of the curve. Moreover, as the displacements are increased, the damage state gets more and more severe throughout the RC wall. The stability of the hysteresis curve and energy dissipation decrease progressively as the amplitude is increased. The specimen exhibited different shear forces for the same displacement level in positive and negative directions, as shown in Figure 7a. In the negative direction, the shear force demand was higher. This is because the specimen was more damaged during the hybrid tests in the positive direction compared to the negative direction; thus, in the negative direction the specimen exhibited more resistance. For the sake of safety, the imposed lateral displacement was limited to 55 mm (2.5% drift). Figure 8 shows the appearance of the ends of the wall with buckling of the external reinforcements in boundary elements and concrete crushing at the end of the pushover test.

### Displacement ductility

Displacement ductility ( $\mu_{\Delta}$ ) is defined as the ratio of the maximum horizontal displacement at the control point ( $\Delta_{max}$ ) and the horizontal displacement of the same point corresponding to yielding of the reinforcement in flexure at the base of the RC wall ( $\Delta_y$ ) [12, 13]:

$$\mu_{\Delta} = \frac{\Delta_{max}}{\Delta_y} \quad (2)$$

To calculate  $\Delta_y$ , a line parallel to the unloading slope of the base moment-displacement hysteresis curve and passing by the origin was graphed as depicted in Figure 8. The yield moment obtained by the MNPhi programme [14] is equal to 1000 kN.m., and during the hybrid tests, the first plastic excursion occurred when the base moment reached 823 kN.m. To avoid overestimating the displacement ductility, the theoretical prediction was chosen as a reference. The yield displacement  $\Delta_y$  is estimated to be 9.83 mm, corresponding to a yield rotation equal to 0.0052 rad. Consequently, using Eq. (2), the maximum displacement ductility that the RC wall experienced was 5.6. This ductility level is higher than the ductility-related force modification factor  $R_d$  equal to 3.5 for which this shear wall was designed using the National Building Code of Canada, 2015 edition [8].

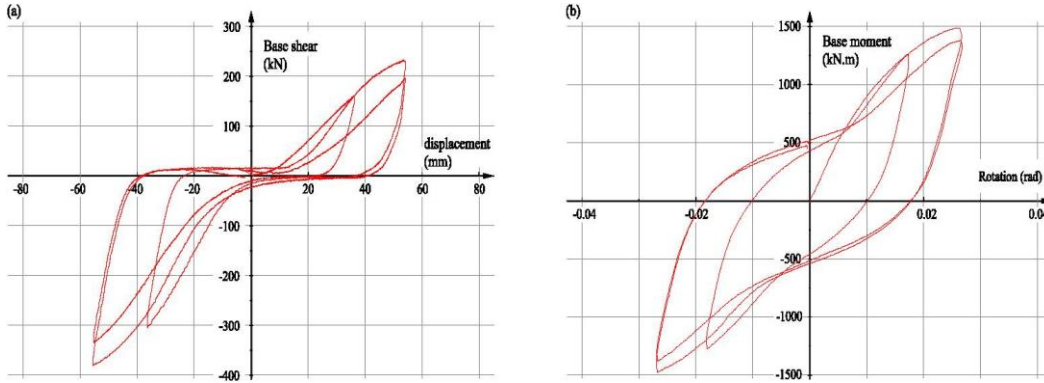


Figure 7. Pushover test results: a) base shear force demand; and b) flexural moment demand.



Figure 8. Bar buckling and loose broken concrete of the RC wall after the pushover test.

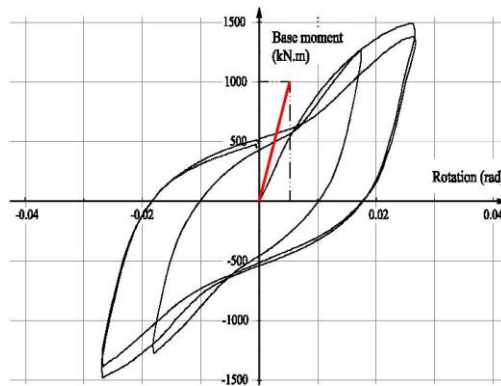


Figure 9. Extracting the rotation corresponding to development of the yielding moment at the wall base.

## CONCLUSIONS

Three successive pseudo-dynamic hybrid tests were performed on an eight-storey RC shear wall to investigate the effect of higher modes on the nonlinear dynamic response at the base of the RC wall. During each successive test, the intensity of the ground motion was increased. As expected, under the design ground motion GM1, yielding occurred in the longitudinal reinforcement at the base of the wall, spreading over a length larger than  $\ell_w/2$ , and thereby forming a plastic hinge. Some horizontal reinforcement yielded due to shear force amplification induced by higher modes. The yielding of the bars was accompanied by major horizontal and diagonal cracks. The shear demand observed during the GM1 hybrid test was 2.27 times greater than the designed expected shear as evaluated, using the capacity design procedure presented in CSA A23.3-14 standard. Under the GM2 ground motion, which had a PGA twice as high as GM1, more yielding was observed, especially in the horizontal reinforcement. The yielding of the bars was also accompanied by severe horizontal and diagonal cracks. The amplified shear demand observed during the GM2 test was 3.01 times greater than the capacity-design value obtained using the CSA A23.3-14 design standard. Test results showed that the dynamic amplification factor for the design shear force addressed in the CSA A23.3-14 is lower than the reality for this particular test specimen. Despite the higher amplification of the base shear force, no shear failure was observed. It seems that the Canadian standard A23.3-14 underestimates the contribution of concrete in shear resistance of reinforced concrete shear walls. The RC wall displacements were decomposed into four different deformation mechanisms: sliding, rotation due to pull-out of longitudinal bars, shear, and flexural deformations. Analysing the contribution of each mechanism in total displacement revealed that at the time of higher shear demand, shear displacement governs the behaviour of the RC wall. After the hybrid tests, the final pushover test demonstrated that the tested RC shear wall can reach displacement ductility levels as large as five.

## ACKNOWLEDGMENTS

The authors gratefully acknowledge the financial support of the Natural Science and Engineering Research Council of Canada and the *Fond de recherche du Québec - Nature et technologies*. Support from the Centre de recherche en génie parasismique et en dynamique des structures (CRGP) of the University of Sherbrooke is also acknowledged. The authors wish to thank Claude Aubé, Jason Desmarais, Éric Beaudoin and Raphaël Prévost, technicians at the University of Sherbrooke who participated in the testing programme. Gabriel Rivard and Wilsonne François helped during the tests.

## REFERENCES

- [1] Filiatrault, A., D'Aronco, D., and Tinawi, R. (1994). "Seismic demand of ductile cantilever walls: a Canadian code perspective". *Canadian Journal of Civil Engineering*, 21, 263–376.
- [2] Tremblay, R., Léger, P., and Tu, J. (2001). "Inelastic seismic response of concrete shear walls considering p-delta effects". *Canadian Journal of Civil Engineering*, 28, 640–655.
- [3] Amaris, A. D. (2002). *Dynamic amplification of seismic moments and shear forces in cantilever walls*. Mémoire de Maîtrise., European School of Advanced Studies in Reduction of Seismic Risk, Italy.
- [4] Panneton, M., Léger, P., and Tremblay, R. (2006). "Inelastic analysis of a reinforced concrete shear wall building according to the National Building Code of Canada 2005". *Canadian Journal of Civil Engineering*, 33, 854–871.
- [5] Boivin, Y., and Paultre, P. (2010). "Seismic performance of a 12-story ductile concrete shear wall system designed according to the 2005 National Building Code of Canada and the 2004 Canadian Standard Association standard A23.3-04". *Canadian Journal of Civil Engineering*, 37(1), 16.
- [6] Boivin, Y., and Paultre, P. (2012). "Seismic force demand on ductile reinforced concrete shear walls subjected to Western North America ground motions: Parametric study". *Canadian Journal of Civil Engineering*, 39, 723–737.
- [7] McKenna, F., Fenves, G., Filippou, F.C., Scott, M., Elgamal, A., Yang, Z., Lu, J., Arduino, P. McKenzie, P., Deierlein, G., and Law, K. (2006). Open system for earthquake engineering simulation (OpenSees), <http://opensees.berkeley.edu>
- [8] National Research Council of Canada - NRCC (2015). National Building Code of Canada; *Part 4: Structural Design*. Canadian Commission on Building and Fire Codes, Ottawa, Ont.
- [9] Canadian Standard Association - CSA (2014). *CAN/CSA-A23.3: Design of concrete structures*. Toronto, ON.
- [10] Atkinson, G.M. (2009). "Earthquake time histories compatible with the 2005 national building code of Canada uniform hazard spectrum". *Canadian Journal of Civil Engineering*, 36, 991– 1000.
- [11] Whyte, C.A., and Stojadinovic, B. (2013). *Hybrid simulation of the seismic response of squat reinforced concrete shear walls*. Report No. PEER 2013/02, Earthquake Engineering Research Center, University of California, Berkeley, CA.
- [12] Mitchell, D., and Paultre, P. (1994). "Ductility and overstrength in seismic design of reinforced concrete structures". *Canadian Journal of Civil Engineering*, 6(21), 1049–1060.
- [13] Mousseau, S., and Paultre, P. (2008). « Seismic performance of a full-scale reinforced high performance concrete building. Part I: Experimental study". *Canadian Journal of Civil Engineering*, 35, 832–848.
- [14] Paultre, P., (2000). WMNPhi; A Sectional Analysis Software for Reinforced Concrete. Université de Sherbrooke, Sherbrooke, Canada.